

LETTER

Compressed ultrafast photography by multi-encoding imaging

To cite this article: Chengshuai Yang *et al* 2018 *Laser Phys. Lett.* **15** 116202

View the [article online](#) for updates and enhancements.



IOP | ebooks™

Bringing you innovative digital publishing with leading voices to create your essential collection of books in STEM research.

Start exploring the [collection](#) - download the first chapter of every title for free.

Letter

Compressed ultrafast photography by multi-encoding imaging

Chengshuai Yang¹, Dalong Qi¹, Jinyang Liang², Xing Wang³,
Fengyan Cao¹, Yilin He¹, Xiaoping Ouyang⁴, Baoqiang Zhu⁴,
Wenlong Wen³, Tianqing Jia¹, Jinshou Tian³, Liang Gao⁵, Zhenrong Sun¹,
Shian Zhang^{1,6,8} and Lihong V Wang^{7,8}

¹ State Key Laboratory of Precision Spectroscopy, East China Normal University, 3663 North Zhongshan Road, Shanghai 200062, People's Republic of China

² Centre Énergie Matériaux Télécommunications, Institut National de la Recherche Scientifique, 1650 boulevard Lionel-Boulet, Varennes, QC J3X1S2, Canada

³ Key Laboratory of Ultra-fast Photoelectric Diagnostics Technology, Xi'an Institute of Optics and Precision Mechanics, Chinese Academy of Sciences, Xi'an 710119, People's Republic of China

⁴ Joint Laboratory on High Power Laser and Physics, Shanghai Institute of Optics and Fine Mechanics, Chinese Academy of Science, Shanghai 201800, People's Republic of China

⁵ Department of Electrical and Computer Engineering, University of Illinois at Urbana-Champaign, 405 North Mathews Avenue, Urbana, IL 61801, United States of America

⁶ Collaborative Innovation Center of Extreme Optics, Shanxi University, 92 Wucheng Road, Taiyuan 030006, People's Republic of China

⁷ Department of Electrical Engineering, Caltech Optical Imaging Laboratory, Andrew and Peggy Cherng Department of Medical Engineering, California Institute of Technology, 1200 East California Boulevard, MC 138-78, Pasadena, CA 91125, United States of America

E-mail: sazhang@phy.ecnu.edu.cn (S Zhang) and lihong@caltech.edu (L V Wang)

Received 5 July 2018

Accepted for publication 31 August 2018

Published 3 October 2018



CrossMark

Abstract

Imaging ultrafast dynamic scenes has been long pursued by scientists. As a two-dimensional dynamic imaging technique, compressed ultrafast photography (CUP) provides the fastest receive-only camera to capture transient events. This technique is based on three-dimensional image reconstruction by combining streak imaging with compressed sensing (CS). However, the image quality and the frame rate of CUP are limited by the CS-based image reconstruction algorithms and the inherent temporal and spatial resolutions of the streak camera. Here, we report a new method to improve the temporal and spatial resolutions of CUP. Our numerical simulation and experimental verification show that by using a multi-encoding imaging method, both the image quality and the frame rate of CUP can be significantly improved beyond the intrinsic technical parameters. Importantly, the temporal resolution by our scheme can break the limitation of the streak camera. Therefore, this new technology has potential benefits in many applications that require the ultrafast dynamic scene image with high temporal and spatial resolutions.

Keywords: ultrafast imaging, computational imaging, imaging reconstruction

(Some figures may appear in colour only in the online journal)

⁸ Author to whom any correspondence should be addressed.

1. Introduction

To observe the temporal and spatial evolutions of ultrafast dynamic scenes, it is critical to capture each frame in the dynamic scene by a specific detection device. Typically, the imaging technologies based on the charge coupled device (CCD) or the complementary metal oxide semiconductor (CMOS) have enabled frame rates of up to 10^7 frames per second (fps) [1]. However, due to the inherent limitations of on-chip storage and electronic readout speed, it is a big challenge to further increase the frame rate, which greatly restricts the applications of these technologies in faster dynamic scene imaging. The pump-probe measurement method can provide a much higher frame rate without the requirement of ultrafast detectors [2–4]. However, this method requires that the dynamic scene must be precisely repeatable. Moreover, this method needs ultrafast probe pulses to provide active illumination. Recently, the advent of compressed ultrafast photography (CUP) overcomes these technical limitations [5]. Compared to the electronic imaging with CCD or CMOS, CUP has an advantage; it can measure transient events with the frame rate of 10^{11} fps in a single shot. So far, CUP has been successfully applied to imaging a number of fundamental ultrafast optical phenomena [5, 6], including the laser pulse reflection and refraction, the photon racing in two media, and the photonic Mach cone. Considering its unique advantages, CUP can be coupled to a variety of imaging modalities in future studies such as microscopes or telescopes. Thus, the object size to be observed can vary from cells to galaxies.

CUP has shown to be a powerful tool to capture transient events. However, there are two inevitable problems. One is the limited image reconstruction quality produced by the compressed sensing (CS) algorithm. The other is that the frame rate is limited by the temporal resolution of the streak camera. Here, we develop multi-encoding CUP to improve both the temporal and spatial resolutions. In CUP, random codes are used to encode the ultrafast dynamic scene and are leveraged to decode the acquired data [5]. In previous studies, hundreds of images were usually reconstructed by single encoding and imaging step. Due to the inherent characteristics of the CS algorithm, the large data compression ratio can be beyond the image reconstruction ability [7–9]. Therefore, a small number of encoding and imaging steps in CUP can limit the image reconstruction quality. Recently, various new technical schemes have been proposed to further improve the image reconstruction quality such as the space and intensity-constrained reconstruction algorithm [10], optimizing the encoding code method [11], and lossless-encoding CUP [6]. However, the improvement is still relatively limited.

In order to show that both the temporal and spatial resolutions of CUP can be significantly improved by the multi-encoding imaging method (i.e. increasing the number of encoding and imaging steps), we numerically simulated a moving Shepp–Logan (S–L) phantom, the superimposition of multiple irrelevant images and a rotating stripe. We also experimentally measured a spatially modulated laser pulse. Our theoretical and experimental results show that a complex dynamic scene can be successfully reconstructed by

multi-encoding CUP, and the temporal resolution can overcome the limitation of the streak camera.

2. Principle

In CUP, an ultrafast dynamic scene $I(x, y, t)$ is spatially encoded by a digital micromirror device (DMD), then temporally sheared in a streak tube, and finally, spatiotemporally integrated by a CCD. The measured image $E(x, y)$ can be mathematically formulated as [5]

$$E(x, y) = \text{TSCI}(x, y, t), \quad (1)$$

where C is the spatially encoding operator, S is the temporally shearing operator, and T is the spatiotemporally integrating operator. To reconstruct the original ultrafast dynamic scene $I(x, y, t)$, equation (1) needs to be inversely solved. A common method is to look for the minimal value of the following object function, which is expressed as [12]

$$f_{\text{TwIST}} = \arg\min \left\{ \frac{1}{2} \|E(x, y) - \text{TSCI}(x, y, t)\|_2^2 + \beta \Phi(I(x, y, t)) \right\}, \quad (2)$$

where β is the regularization parameter, and Φ is the regularization function.

In multi-encoding imaging, as shown in figure 1, an ultrafast dynamic scene is divided into several replicas, and each replica is encoded by a different encoding mask. Finally, these components are individually imaged by a CCD after the temporal shearing. Thus, equation (1) can be further formulated in a matrix form as

$$\begin{bmatrix} E_1(x, y) \\ E_2(x, y) \\ \vdots \\ E_k(x, y) \end{bmatrix} = \begin{bmatrix} \text{TSC}_1 \\ \text{TSC}_2 \\ \vdots \\ \text{TSC}_k \end{bmatrix} I(x, y, t), \quad (3)$$

where k is the number of encoding and imaging steps. In the image reconstruction by the TwIST algorithm, we perform the following operation in each iteration,

$$\tilde{I}^n(x, y, t) = \sum_{m=1}^k (C_m)^T (\text{TS})^T \tilde{E}_m^n(x, y), \quad (4)$$

where n represents the n th iteration. In each iteration, the image information includes the signal and noise components. The signals in each measurement are relevant, while the noises are not. Thus, the signal to noise ratio (SNR) can be increased by using the multi-encoding imaging method. This approach is similar to the weak signal measurement by the synchronous accumulation method [13]. Since the SNR in each iteration can be increased, the final image quality can be improved.

In CS-based image reconstruction, the measurement error δ between reconstructed ($I^\#(x, y, t)$) and original ($I(x, y, t)$) ultrafast dynamic scenes obeys the relationship [7]

$$\delta = \left\| I(x, y, t) - I^\#(x, y, t) \right\|_2 \leq C \cdot R \cdot (M \cdot k / \log N)^{-(1/p-1/2)}, \quad (5)$$

where C and R are constants that are correlated with ($I(x, y, t)$), M and N are the numbers of elements in x and y

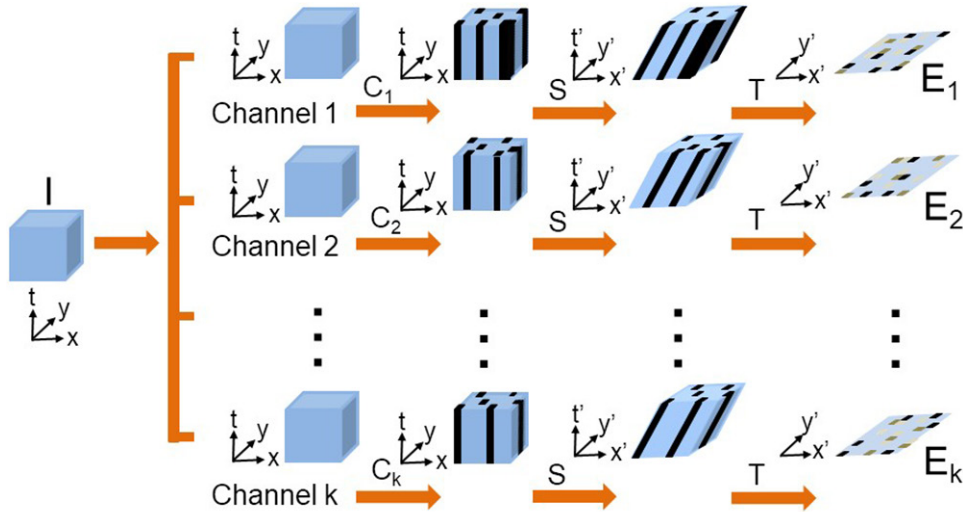


Figure 1. The schematic diagram of data acquisition for multi-encoding CUP. Here, t, t' : time; x, y : spatial coordinates of the dynamical scene; x', y' : spatial coordinates at the streak camera; C_k : spatially encoding operator; S : temporally shearing operator; and I : spatiotemporally integration operator.

axes of $E(x, y)$ and $I(x, y, t)$, and p is a value in the range of 0 to 1 (i.e. $0 < p < 1$). It is easy to verify from equation (5) that a larger number of encoding and imaging steps (k) will lead to a smaller measurement error δ . That is, with an increase in the number of encoding and imaging steps (k), the reconstructed dynamic scene will approach to the original dynamic scene. Usually, the reconstructed dynamic scene can be considered to be acceptable when the number of encoding and imaging steps (k) satisfies the following relationship [7, 9, 14]

$$k > F \cdot S \cdot \mu^2, \quad (6)$$

where F is constant that is correlated with the element numbers N and M , S is a nonzero number in θ , where $\theta = \Psi^{-1}I$ and Ψ is the sparsifying basis. μ is the mutual coherence, which is defined as [7]

$$\mu = \sqrt{N} \max_{i,j} \langle O_i, \Psi_j \rangle, \quad (7)$$

where O is the basis measurement with $O = TSC$. Here, O and Ψ are discrete matrices by transforming a 3D datacube into 2D data. Equation (5) indicates that the image reconstruction accuracy is proportional to the number of encoding and imaging steps k , while equations (6) and (7) give the criterion for successful image reconstruction. Generally, the dynamic scene with the lower sparsity needs a larger number of encoding and imaging steps to be well reconstructed. In principle, any complex dynamic scene can be successfully reconstructed by increasing the number of encoding and imaging steps (k).

As shown in equation (5), increasing the number of encoding and imaging steps can improve the image reconstruction accuracy, which manifests as the improvement of spatial and temporal resolutions. In theory, CUP's spatial and temporal resolutions are usually determined by one DMD's pixel size. In the actual CUP system, the temporal resolution is further deteriorated by the streak camera to multiple DMD pixels in imaging. In mathematics, the temporal resolution of the streak camera can be written as [15]

$$\tau = \frac{1}{\zeta \eta}, \quad (8)$$

where η is the spatial resolution of the streak camera ($\eta \propto 1/\Delta z$, Δz is the distinguishable pixel size), and ζ is the constant that is related to the sweep voltage of the streak camera. Owing to multi-encoding imaging (i.e. increasing the number of encoding and imaging steps, k), the temporal resolution can overcome the limitation of the streak camera. This approach is similar to the working principle of a single-pixel camera [16–18], where a single-pixel detector can measure a two-dimensional image by multiple measurements based on image encoding and decoding.

3. Numerical simulation

We first show that CUP's spatial resolution can be improved by multi-encoding imaging. Below we numerically simulated two dynamic scenes. The first dynamic scene is a moving 200-by-200 S–L phantom. The S–L phantom moved from left to right with ten pixels per frame, and the whole dynamic scene contained nine frames. The original image and reconstructed results are shown in figures 2(a) and (b), respectively. To quantitatively assess the image reconstruction quality, we calculated the peak signal to noise ratio (PSNR) by comparing the original and reconstructed images as shown in figure 2(c). With an increase in the number of encoding and imaging steps, the PSNR value shows a fast increase followed by a slow increase. When the number of encoding and imaging steps is increased to 15, the PSNR value can be up to 41.79, which is considered high quality in many applications [19]. The second dynamic scene is the superimposition of multiple irrelevant images. Here, nine completely different images were spatially superimposed and formed a complex dynamic scene with less sparsity compared to the moving S–L phantom. Figure 3(a) shows the original image together

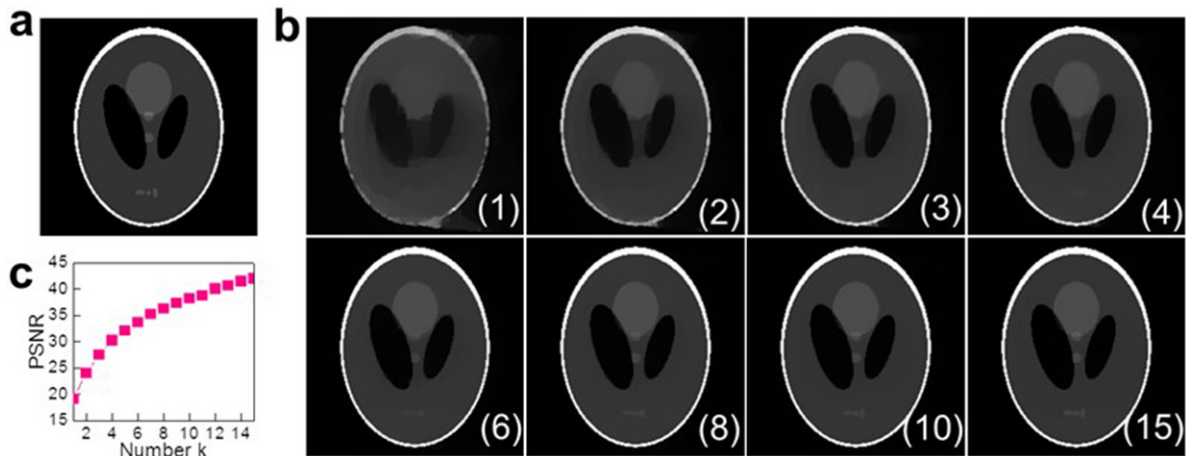


Figure 2. Numerical simulation results of moving the S–L phantom from left to right. (a) The original S–L phantom image; (b) the reconstructed images by 1, 2, 3, 4, 6, 8, 10, and 15 encoding and imaging steps; (c) the PSNR values versus the number of encoding and imaging steps, k .

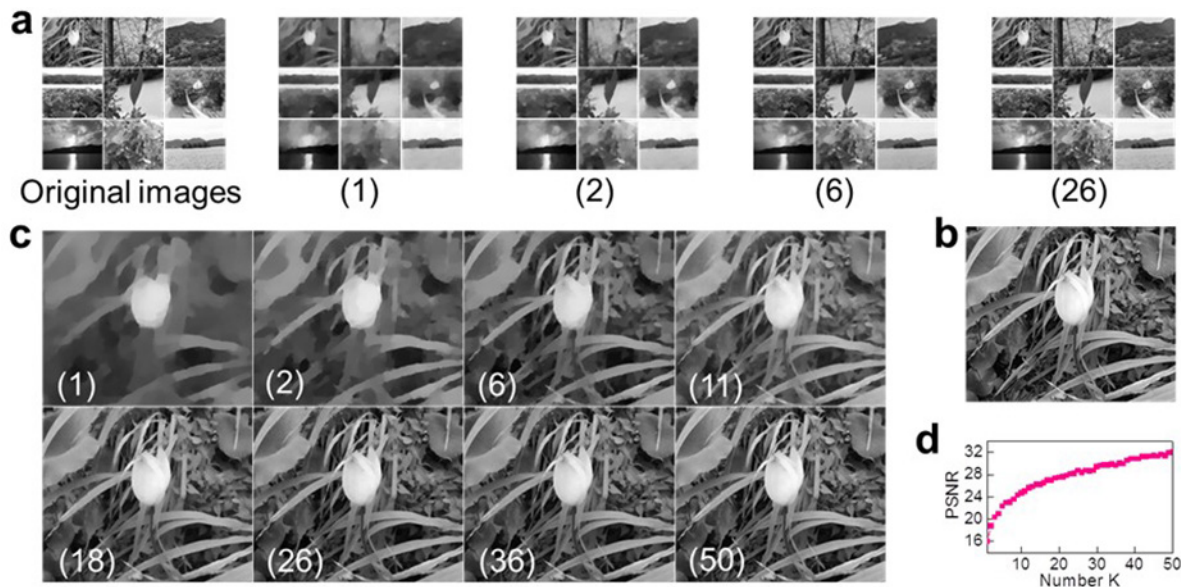


Figure 3. Numerical simulation results of the superimposition of nine irrelevant images. (a) The reconstructed nine images by 1, 2, 6, and 26 encoding and imaging steps together with original nine images; (b) a selected original image; (c) the reconstructed images by 1, 2, 6, 11, 18, 26, 36, and 50 encoding and imaging steps; (d) the PSNR values versus the number of encoding and imaging steps, k .

with the reconstructed images. After 26 encoding and imaging steps, all nine images can be reconstructed. To clearly observe the image reconstruction effect, we picked the first image for comparison. The original and reconstructed images are respectively shown in figures 3(b) and (c), and the calculated PSNR values are given in figure 3(d). The dynamic scene is complex, but it can still be reconstructed by increasing the number of encoding and imaging steps. The two simulation results verified that the complex dynamic scenes can be successfully measured by multi-encoding CUP.

Next, we demonstrate that the multi-encoding CUP can improve the temporal resolution over that of the streak camera. Here, we numerically simulated the stripe rotation. The stripe rotated 180° in the space; 10° in each frame. Therefore, the whole dynamic scene contained eighteen frames. The spatial resolution was set to be 3×3 pixels on CCD. Thus, the intrinsic temporal resolution should be no better than three

pixels. However, we used one pixel size of DMD to reconstruct the dynamic scene. Here, image sizes on DMD and CCD were set to be the same, and the pixel sizes and numbers for DMD and CCD were also the same. Figures 4(a1) and (a2) show the original image and the simulated image with a limited resolution. Figures 4(b)–(e) show the image reconstruction results using 1, 2, 6, and 30 encoding and imaging steps. For the smaller numbers of encoding and imaging steps, as shown in figures 4(b) and (c), the image reconstruction quality is relatively poor (see figures 4(a3) and (a4)). Moreover, the motion of stripe rotation cannot be distinguished within the adjacent three reconstructed images. Thus, the dynamic information during this evolution is lost. However, with the larger numbers of encoding and imaging steps (see figures 4(d) and (e)), the spatial resolution of reconstructed images is significantly improved (see figures 4(a5) and (a6)). More importantly, the whole rotation process of the stripe can be better

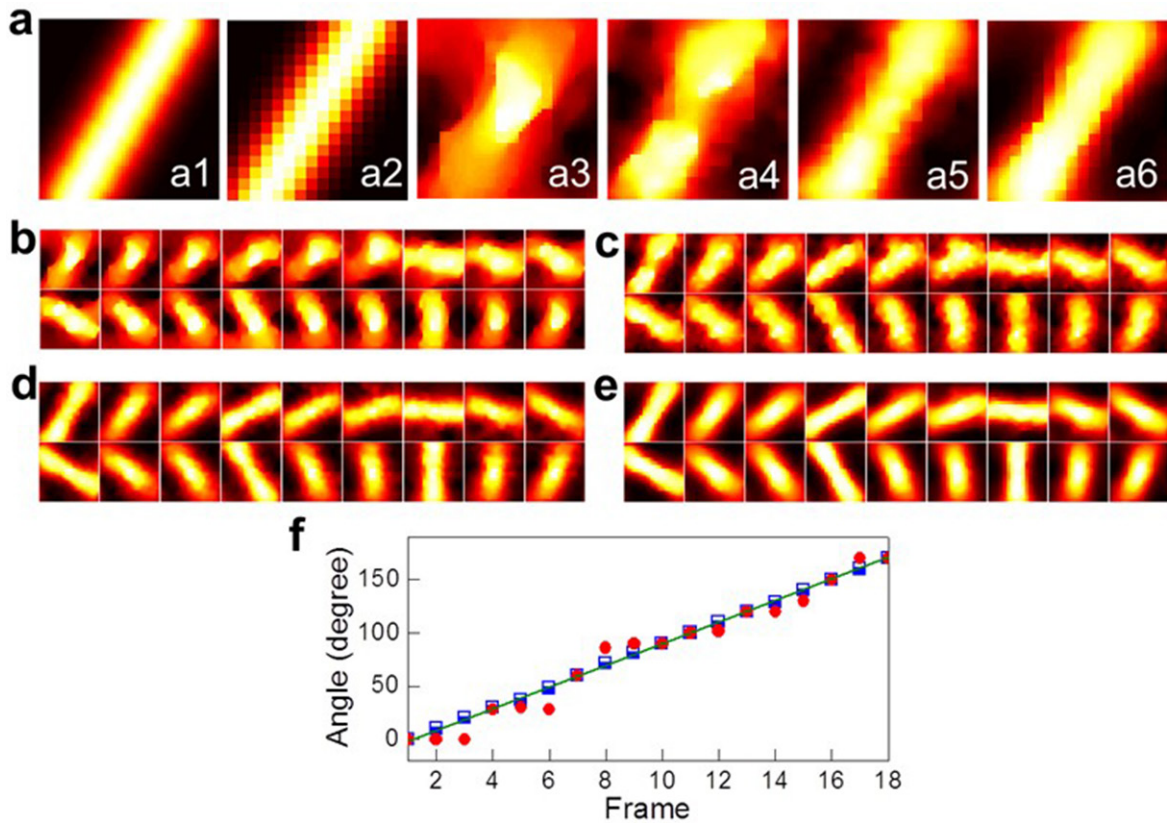


Figure 4. Numerical simulation results of rotating stripe. (a) A selected original image (a1) and the simulated image with a limited resolution (a2) together with the reconstructed images by 1, 2, 6, and 30 encoding and imaging steps (a3)–(a6); (b)–(e) the reconstructed eighteen images by 1, 2, 6, and 30 encoding and imaging steps; (f) the stripe rotation angle in each frame for 1 (circles) and 30 (squares) encoding and imaging steps together with the linear fitting (line).

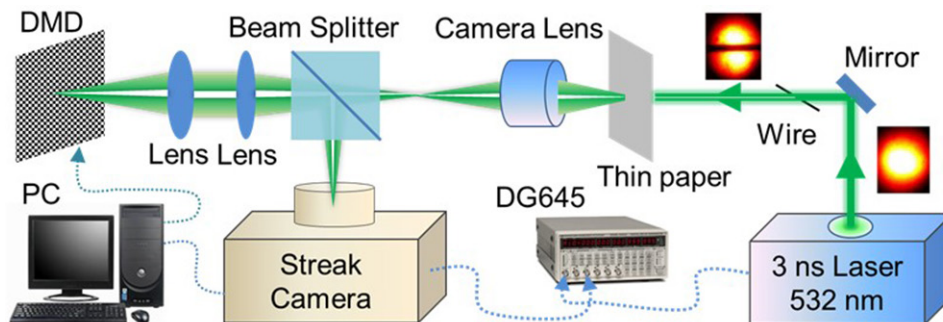


Figure 5. The experimental arrangement for the temporal and spatial measurements of a 3 ns pulsed laser spot by using the multi-encoding CUP system. Here, DMD: digital micromirror device; DG645: digital delay generator; PC: personal computer.

resolved. To illustrate the temporal resolution improvement by the multi-encoding imaging method, we present the stripe rotation angle in each frame by 1 and 30 encoding and imaging steps as shown in figure 4(f). The stripe rotation angle has a linear increase for 30 encoding and imaging steps, which is the same as the original dynamic scene. In comparison, the data from 1 encoding and imaging step are less accurate.

4. Experimental verification

In the multi-encoding CUP experiment, we can employ two methods. One is multiple measurements in a single channel but the dynamic scene must be precisely repeatable. The other

one is single measurement in multiple channels; this method is applicable to various dynamic scenes. To validate our theory, we measured a spatially modulated laser pulse by using the multi-encoding CUP. Because the dynamic scene was repeatable, we adopted the first method for multiple measurements in a single channel. The schematic diagram of experimental arrangement is shown in figure 5. Here, a nanosecond laser (Q-smart 450, Quantel, pulse width of about 3 ns, central wavelength of 532 nm, and repetition rate of 10 Hz) was used in multi-encoding CUP. To obtain a pulsed laser spot with a special spatial structure, we used a thin wire to divide the laser spot into two components in space. The laser spot size was 3 mm in diameter, while the wire size was about 300 μm

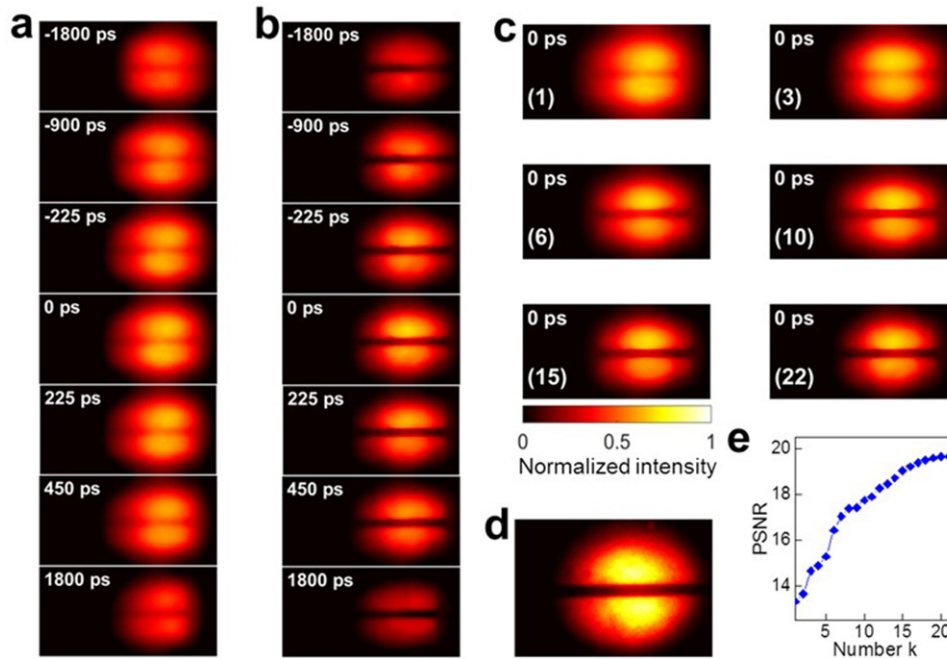


Figure 6. Experimental results of a spatially modulated laser pulse. (a) and (b) The reconstructed images with the temporal resolution of 180 ps by 1 and 22 encoding and imaging steps; (c) the reconstructed images at the time zero by 1, 3, 6, 10, 15, and 22 encoding and imaging steps; (d) the measured pulse laser spot by an external CCD; (e) the PSNR values versus the number of encoding and imaging steps, k .

in diameter. The spatially modulated nanosecond laser spot was projected onto a thin white paper, and a small fraction of photons passed through the white paper. This spatially modulated laser pulse on the white paper was imaged using the multi-encoding CUP. In the system, the dynamic scene was imaged via a camera lens and a 4f imaging system. Then, the image was encoded by a DMD (Texas Instruments). Finally, the encoded image was sent to a streak camera (Model 2200, XIOPM) for measurement. In our CUP system, the temporal resolution of the streak camera was 180 ps, and the spatial resolution was 7.7 lp mm^{-1} .

Figures 6(a) and (b) show the reconstructed images of spatially modulated laser pulse by 1 and 22 encoding and imaging steps. Seven representative images were chosen to display. The time interval between two adjacent reconstructed images was set to be 180 ps, which is equal to the temporal resolution of the streak camera. In this case, the time evolution process of a pulsed laser spot can be clearly observed by both 1 and 22 encoding and imaging steps, while the latter shows the higher image reconstruction quality. Especially, the blocked center part by the thin wire in the laser spot can be clearly displayed by multi-encoding CUP. To show the improvement of the reconstructed image quality by increasing the number of encoding and imaging steps, we picked the reconstructed images at time zero for the different numbers of encoding and imaging steps. These selected images are shown in figure 6(c) and together with the static image in figure 6(d) for comparison. Here, the static image was measured by an external CCD. With the increase in the number of encoding and imaging steps, the spatial contour of the reconstructed image gradually approaches the static

image. We also calculated the corresponding PSNR values of these reconstructed images. The calculated results are shown in figure 6(e). As the number of encoding and imaging steps increases, the PSNR value quickly increases and then reaches a plateau. The increase of the PSNR value further confirms that multi-encoding imaging can improve the spatial resolution of CUP.

To show that the multi-encoding imaging can break the limit of temporal resolution of the streak camera, we reconstructed the dynamic scene of the spatially modulated laser pulse with the temporal resolutions of 180, 90, and 45 ps. The reconstructed results for the cases of 1 and 22 encoding and imaging steps are shown in figure 7. Here, we selected five adjacent images with obvious intensity variation to observe. Moreover, to more clearly show the improvement in the temporal resolution, we also plot the corresponding intensities of these reconstructed images in figure 7. As shown in figure 7(a), the temporal resolution of 180 ps corresponds to the limitation of the streak camera, the intensity variation of the pulsed laser spot can be clearly observed by both 1 and 22 encoding and imaging steps. However, with an increase of the temporal resolution, as shown in figures 7(b) and (c), the intensity variation of the pulsed laser spot becomes indistinguishable by 1 encoding and imaging step, while it is still distinguishable by 22 encoding and imaging steps. When the temporal resolution is 45 ps (see figure 7(c)), the five adjacent images by 1 encoding and imaging step have almost identical structure and intensity. It is easy to see that, by multi-encoding imaging, both the temporal and spatial resolutions of CUP can be improved. Most importantly, the temporal resolution can be finer than that of the streak camera.

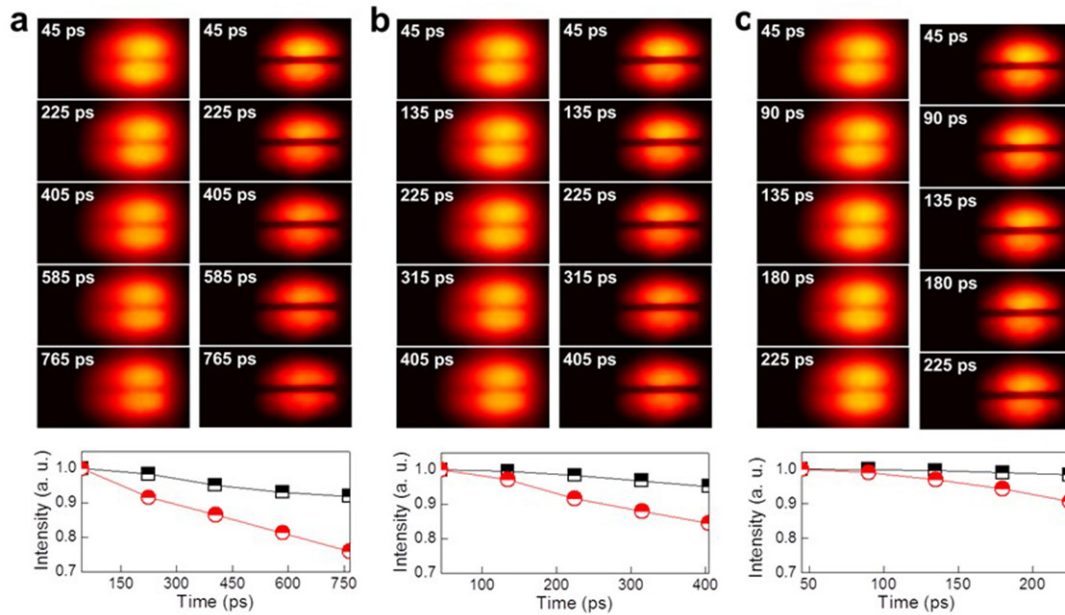


Figure 7. The reconstructed images by 1 (left panels) and 22 (right panels) encoding and imaging steps with the temporal resolutions of 180 (a), 90 (b) and 45 ps (c), together with the corresponding intensity variation for 1 (squares) and 22 (circles) encoding and imaging steps (below panels).

5. Discussion

Multi-encoding imaging has shown to be a well-established strategy to improve the temporal and spatial resolutions of CUP. In the experiment above, we perform multiple measurements with a single channel for the repeatable dynamic scene. To keep the single-shot advantage, we can also use a lenslet array for a single measurement with multiple channels, and each imaging channel is individually encoded by the code mask. The experimental design is shown in figure 8. The photocathode of a streak camera is divided into several parts for imaging. Thus, the disadvantage of this scheme is a reduced spatial resolution. Therefore, it cannot measure the dynamic scene with the complex spatial structure. An alternative method to overcome the defect is to employ multiple streak cameras, which would be costly.

The theory and simulation above have shown that the multi-encoding CUP can measure the complex dynamic scene. However, in order to accurately reconstruct the complex dynamic scene, the number of encoding and imaging steps usually needs to reach a few or even tens. In actual experiments, if the dynamic scene is repeatable, it is proposed to employ the scheme of multiple measurements with a single channel. On one hand, because the DMD is programmable, it is easy to change the encoding mask in each measurement. On the other hand, the whole CUP system is relatively compact, and it is easy to be instrumented in future applications.

Our simulation and experiment have proved that the multi-encoding imaging method can break the temporal resolution limit of the streak camera. As shown in equation (8), the temporal resolution of the streak camera is correlated with the spatial resolution. Due to the performance of the streak camera, the spatial resolution usually covers multiple pixels of the DMD in imaging. That is, it needs to merge multiple pixels

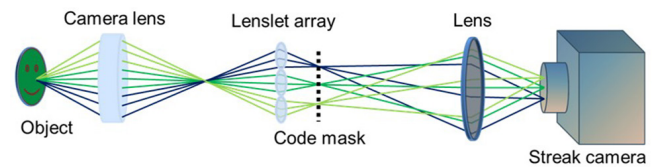


Figure 8. The schematic diagram of a multi-encoding CUP system by a single measurement with multiple channels based on the lenslet array.

of the DMD to obtain a clear encoded image. However, in the image reconstruction, one pixel size of the DMD is usually used to determine the maximal temporal resolution. If a smaller pixel size is used, more pixels are covered under the same spatial resolution of the streak camera. Thus, the temporal resolution will be higher. Generally, the pixel size should be determined under the optical diffraction limit. In future experiments, we can use a smaller DMD pixel size in CUP imaging. Therefore, using the picosecond streak camera can potentially image the femtosecond dynamic process by multi-encoding CUP.

6. Conclusions

In summary, we have developed a multi-encoding imaging method to improve the image reconstruction accuracy of CUP. Here, both the temporal and spatial resolutions can be significantly improved by increasing the number of encoding and imaging steps. Our results showed that this multi-encoding CUP can capture complex dynamic scenes. Most importantly, the temporal resolution can be finer than that of the streak camera. This study can advance the CUP technique to a new level and may promote its practical applications in ultrafast imaging. Furthermore, based on multiple measurements, our

method can be applied to imaging dynamic scenes with weak signal levels for future studies.

Acknowledgments

This work was partly supported by the National Natural Science Foundation of China (No. 11727810 and No. 11774094) and Science and Technology Commission of Shanghai Municipality (No. 17ZR146900 and No. 16520721200).

Author contributions

C Yang wrote the program, performed the experiments, analyzed the data, and prepared the manuscript. D Qi built the experimental system and analyzed the data. J Liang wrote a part of the program and revised the manuscript. X Wang performed some of the experiments and analyzed the data. F Cao performed some of the experiments. Y He also performed some of the experiments. X Ouyang performed some of the experiments as well. B Zhu contributed to the experimental design. W Wen performed some of the theoretical calculations. T Jia analyzed the data. J Tian contributed to the experimental design. Z Sun contributed to the data analysis and manuscript revision. L Gao contributed to the manuscript revision. S Zhang contributed to the experimental design, image reconstruction, data analysis and manuscript revision. L Wang contributed to the conceptual system and manuscript revision.

Competing interests

The authors declare that they have no competing financial interests.

References

- [1] Kondo Y, Takubo K and Tominaga H 2012 Development of 'HyperVision HPV-X' high-speed video camera *Shimadzu Rev.* **69** 285–91
- [2] Velten A, Willwacher T, Gupta O, Veeraraghavan A, Bawendi M G and Raskar R 2012 Recovering three-dimensional shape around a corner using ultrafast time-of-flight imaging *Nat. Commun.* **3** 745
- [3] Gariepy G, Krstajić N, Henderson R, Li C, Thomson R R, Buller G S, Heshmat B, Raskar R, Leach J and Faccio D 2015 Single-photon sensitive light-in-flight imaging *Nat. Commun.* **6** 6021
- [4] Hockett P, Bisgaard C Z, Clarkin O J and Stolow A 2011 Time-resolved imaging of purely valence-electron dynamics during a chemical reaction *Nat. Phys.* **7** 612–5
- [5] Gao L, Liang J, Li C and Wang L V 2014 Single-shot compressed ultrafast photography at one hundred billion frames per second *Nature* **516** 74–7
- [6] Liang J, Ma C, Zhu L, Chen Y, Gao L and Wang L V 2017 Single-shot real-time video recording of a photonic Mach cone induced by a scattered light pulse *Sci. Adv.* **3** e1601814
- [7] Candes E J and Tao T 2006 Near-optimal signal recovery from random projections: universal encoding strategies? *IEEE Trans. Inf. Theory* **52** 5406–25
- [8] Candès E J, Romberg J and Tao T 2006 Robust uncertainty principles: exact signal reconstruction from highly incomplete frequency information *IEEE Trans. Inf. Theory* **52** 489–509
- [9] Candès E J, Romberg J K and Tao T 2006 Stable signal recovery from incomplete and inaccurate measurements *Commun. Pure Appl. Math.* **59** 1207–23
- [10] Zhu L, Chen Y, Liang J, Xu Q, Gao L, Ma C and Wang L V 2016 Space- and intensity-constrained reconstruction for compressed ultrafast photography *Optica* **3** 694–7
- [11] Yang C et al 2018 Optimizing codes for compressed ultrafast photography by genetic algorithm *Optica* **5** 147–51
- [12] Bioucas-Dias J M and Figueiredo M A 2007 A new TwIST: two-step iterative shrinkage/thresholding algorithms for image restoration *IEEE Trans. Image Process.* **16** 2992–3004
- [13] Klein M P and Barton G W 1963 Enhancement of signal-to-noise ratio by continuous averaging: application to magnetic resonance *Rev. Sci. Instrum.* **34** 754–9
- [14] Abolghasemi V, Ferdowsi S, Makkiabadi B and Sanei S 2010 On optimization of the measurement matrix for compressive sensing *Signal Processing Conf.* pp 427–31
- [15] Chang Z et al 1996 Demonstration of a sub-picosecond x-ray streak camera *Appl. Phys. Lett.* **69** 133–5
- [16] Duarte M F, Davenport M A, Takbar D, Laska J N, Sun T, Kelly K F and Baraniuk R G 2008 Single-pixel imaging via compressive sampling *IEEE Signal Process. Mag.* **25** 83–91
- [17] Arce G R, Brady D J, Carin L, Arguello H and Kittle D S 2014 Compressive coded aperture spectral imaging: an introduction *IEEE Signal Process. Mag.* **31** 105–15
- [18] Arguello H, Rueda H and Arce G R 2012 Spatial super-resolution in code aperture spectral imaging *SPIE Conf. Defense, Security and Sensing* p 83650A
- [19] Orsdemir A, Altun H O, Sharma G and Bocko M F 2008 On the security and robustness of encryption via compressed sensing *Military Communications Conf.* pp 1–7